crystals

MDPI

Article

Synthesis of Thiophene-Based Derivatives and the Effects of Their Molecular Structure on the Mesomorphic Behavior and Temperature Range of Liquid-Crystalline Blue Phases

Meng Wang [1,*], He Song [1], Chongye Wu [1], Beiqi Liu [1], Zichen Wang [2] and Huai Yang [2,*]

[1] Department of Materials Science and Engineering, School of Mechanical Electronic and Information Engineering, China University of Mining and Technology-Beijing, Beijing 100083, China
[2] Beijing Advanced Innovation Center for Materials Genome Engineering, School of Materials Science and Engineering, Peking University, Beijing 100871, China
* Correspondence: 201823@cumtb.edu (M.W.); yanghuai@pku.edu.cn (H.Y.)

Abstract: The development of blue-phase liquid crystal (BPLC) materials with a wide temperature range is of great significance for practical applications in the optoelectronic field. In the study, bent-core derivatives with a 3-hexyl-2,5-disubstituted thiophene central ring in the λ-shaped molecular structure were designed and synthesized. Their mesomorphic behavior and effect on the blue-phase (BP) temperature range were investigated. Interestingly, a BP was achieved both during the heating and cooling processes by doping with a proper concentration of chiral compound into the thiophene bent-shaped molecule with high rigidity, while derivatives with fluorine atom substitution only exhibited cholesteric phase no matter how many chiral compounds were added. This result proved that BP is highly sensitive to the molecular structures of bent-shaped molecules. Moreover, the BP temperature range was broadened when adding these molecules into a BPLC host, which thus improved the BP temperature range from the initial value, no more than 4 °C, to as much as 24 °C. The experimental phenomena were reasonably explained through molecular simulation calculations. The study may provide some experimental basis and theoretical guidance for the design of novel bent-shaped molecules and BPLC material with a wide temperature range.

Keywords: blue phase; bent-shaped molecule; 3-hexyl-2,5-disubstituted thiophene; temperature range; phase transition

check for updates

Citation: Wang, M.; Song, H.; Wu, C.; Liu, B.; Wang, Z.; Yang, H. Synthesis of Thiophene-Based Derivatives and the Effects of Their Molecular Structure on the Mesomorphic Behavior and Temperature Range of Liquid-Crystalline Blue Phases. *Crystals* **2023**, *13*, 916. https://doi.org/10.3390/cryst13060916

Academic Editor: Jagdish K. Vij

Received: 13 May 2023
Revised: 1 June 2023
Accepted: 5 June 2023
Published: 6 June 2023

Copyright: © 2023 by the authors. Licensee MDPI, Basel, Switzerland. This article is an open access article distributed under the terms and conditions of the Creative Commons Attribution (CC BY) license (https://creativecommons.org/licenses/by/4.0/).

1. Introduction

Liquid-crystalline blue phases (BPs) have recently drawn vast and increasing attention due to their exotic fluid self-assembled three-dimensional periodic supernanostructures and the characteristic of selective reflection of circularly polarized light in the visible-light range [1]. BPs generally appear in the narrow temperature range close to the isotropic phase (Iso) in a liquid crystal (LC) material system with a high chiral dopant concentration. Unlike the one-dimensional helical twist structure of chiral nematic phase (Ch), the BPs' molecules twist along two different orientation axes, forming a double-twisted cylinder (DTC) arrangement spontaneously. As the double-twisted structure is unable to continuously occupy a three-dimensional space, BPs must coexist with defects. Since the generation of such a defect involves some energy, the entire system becomes unstable. This is the main reason for the poor thermodynamic stability performance of BPs. Depending on the difference in the three-dimensional long-range-ordered assembly structure of the DTCs, BPs are classified into three categories: BP I, BP II, and BP III. These three subphases generally appear in sequence with the increase in temperature or chiral content [2]. It has been revealed that BP II has a simple cubic unit cell of lattice defects and BP I is body-centered cubic, both with lattice parameters in the order of several hundred nanometers and resulting in light reflection in the visible spectrum [3,4]. BP III is amorphous and its symmetry is the

same as that of I [5]. Due to their self-assembly nanostructures and exotic electric–optical characteristics, BPs have recently encouraged enormous interest in the development of functional LC materials and the great potential for advanced applications in a wide variety of fields such as displays, light modulators, photonic materials, tunable lasers, and optical communications [6,7]. However, the extremely narrow existing temperature range of BPs is still one of the most crucial obstructions for practical application [8]. Therefore, new BPLC materials with an inherent broad temperature range has been developed and made significant progress in recent decades.

Due to the exotic self-organized nanostructures, the classical molecular design methods for a conventional LC phase composed of rod-like molecules is inapplicable to BPLC [9]. To develop BP materials with an inherently wide temperature range, extensive investigations have been conducted to design molecules with novel structures or configuration, such as dimer molecules [10,11], T-shaped (also called λ-shaped) molecules [12,13], U-shaped molecules [14], or bent-core molecules [15,16]. Remarkably, bent-shaped or banana molecules have drawn significant attention, as they can exhibit the LC phase with a structural chirality–average molecular direction despite being built from achiral molecules [17,18]. In 2003, Nakata et al. first reported that the BP temperature range was broadened by doping achiral bent-shaped molecules [19]. In 2010, Lee et al. obtained a BPLC material with a temperature range of about 15 °C by doping some percentage of a chiral additive into a simple mixture of bent-shaped molecules exhibiting the nematic phase [20]. Moreover, numerous research works have reported that doping bent-shaped molecules can significantly increase the temperature range of a small-molecule BPLC material system [21–26]. Bent-shaped molecules are considered to possess biaxiality, which help the coupling with chirality and lead to the shrinkage of defect cores [27]. Thus, the double-twisted arrangement can be enhanced and the BP can be stabilized [28]. Through the doping of the bent-shaped molecules with photoisomeric functional groups, the BPLC can also exhibit excellent light-induced color variance or photoinduced phase transition performances [29,30]. After years of innovative research, it has been proven that the molecular structures and functional groups of the bent-shaped molecules play a decisive role in the performance of the BP mixtures [31–33]. To date, different compounds with 2,5-disubstituted furan, 2,5-disubstituted pyrrole, 2,5-disubstituted oxadiazole, or 1,3-disubstituted benzene ring as the core structure have been successfully synthesized and used to stabilize the blue-phase temperature range [9,34–37]. Among them, the bending angle of compounds with 2,5-disubstituted thiophene is about 154°, which is larger than that of other common ring centers as mentioned above [23]. It may be easy to form a molecular twisted configuration and improve biaxiality. To investigate the effects of the molecular structures on the mesomorphic behavior and BP temperature, a series of thiophene bent-core derivatives in a λ-shaped molecular structure were designed and synthesized by introducing different rigid structures and side substitution groups on the 3-hexyl-2,5-disubstituted thiophene central ring in this study. Simulation calculations of optimizing the molecular configuration and the corresponding structural parameters were also carried out to explain the experimental phenomena.

2. Results and Discussion

Four symmetrically 2,5-disubstituted thiophene derivatives (Figure 1) used in this study were prepared according to Scheme S1. The chiral dopant R811 and Iso-(6OBA)$_2$ (Figure S6) were obtained from Shijiazhuang Slichem Display Material Co., Ltd. Beijing, China. The biphenyl carboxylic acids (98% purity) used in the study were obtained from Beijing Bayi Space Lcd Technology Co., Ltd. Beijing, China. The chemical structures of the synthesized compounds were identified with an ^{1}H NMR (Bruker HW-400, Karlsruhe, Germany) and FT-IR spectrometer (Perkin-Elmer, Spectrum 100, Waltham, MA, USA). The ^{1}H NMR spectrum of C6O-6Th, C5PP-6Th, C5PPF(2)-6Th and C5PPF(3)-6Th can be found in supplementary materials (Figures S1–S4). The temperatures and enthalpies of the transition were investigated using differential scanning calorimetry (DSC) (PerkinElmer,

DSC8000, Waltham, MA, USA) at a scanning rate of 10.0 °C min^{-1} under a dry nitrogen purge. The initial phase assignments and corresponding transition temperatures for the final compounds were determined by using thermal optical microscopy with a polarizing microscope (POM) (Carl Zeiss, AxioVision SE64, Oberkohen, Germany) equipped with a hot stage calibrated to an accuracy of ±0.1 °C (Linkam LTS420, Salfords, United Kingdom). The LC cells used in the study were made with indium-tin-oxide (ITO)-coated glass substrates with no inner surface treatment or parallel treatment. The thickness were controlled to be approximately 20 μm by poly(ethylene terephthalate) film. The BP textures were identified under the reflection (R)-mode POM. The reflection spectra were measured by using a reflection-type optical fiber spectrometer (AvaSpec-ULS2048, Avantes China, Beijing, China).

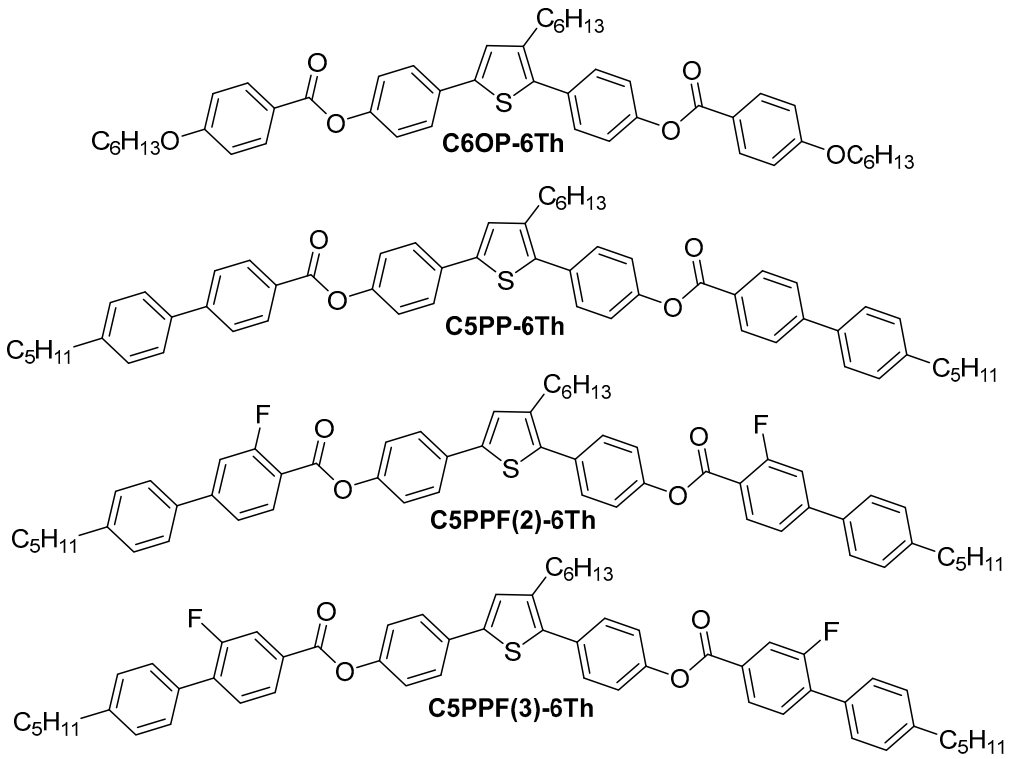

Figure 1. Chemical structures of the 2,5-disubstituted thiophene derivatives with different terminal groups and lateral substituents.

2.1. Mesomorphic Behavior

The thermotropic liquid-crystalline behaviors were examined using POM and DSC. The DSC curves for the compounds in the initial cooling and subsequent heating processes are presented in Figure S5. The phase transition temperatures and enthalpy changes for the compounds were derived from the DSC measurements and are shown in Table 1. The POM textures of this series of bent-shaped molecules during the cooling cycle at different temperatures are shown in Figure 2. By combining the POM typical textures and DSC test results, the mesomorphic behaviors are summarized in Table 1. It can be seen that compound C6OP-6Th showed no mesophases but, surprisingly, a low melting point of about 59.4 °C. By comparison, compounds C5PP-6Th, C5PPF(2)-6Th, and C5PPF(3)-6Th exhibited nematic phase with differences in the phase transition temperature. It could be supposed that the λ-shaped molecules exhibited the LC phase by increasing the rigid structures of the side substitution groups on the 3-hexyl-2,5-disubstituted thiophene central ring [38]. By the lateral F moiety situated around the ester linkage of the molecular skeleton, the phase transition temperatures from the crystal state to nematic phase were decreased.

Moreover, the position of -F also mattered, especially its ortho-substitution, which dropped the clearing point temperature by more than 30 °C.

Table 1. The phase transition temperature and corresponding transition enthalpies of the thiophene-based λ-shaped molecules during initial cooling and subsequent heating cycles.

Compound	Cooling Cycle/(°C, ΔH/J g^{-1})	Heating Cycle (°C, ΔH/J g^{-1})
C6OP-6Th	Iso 59.4 (48.1) Cr	Cr 84.4 (47.9) Iso
C5PP-6Th	Iso 262.2 (2.3) N 100.1 (34.3) Cr	Cr 126.4 (40.2) N 265.2 (2.8) Iso
C5PPF(2)-6Th	Iso 230.0 (0.9) N 82.5 (21.3) Cr	Cr 104.2 (22.8) N 232.7 (1.0) Iso
C5PPF(3)-6Th	Iso 262.0 (1.2) N 95.0 (23.2) Cr	Cr 107.0 (24.6) N 266.7 (1.0) Iso

Cr: crystal; N: nematic phase; Iso: isotropic.

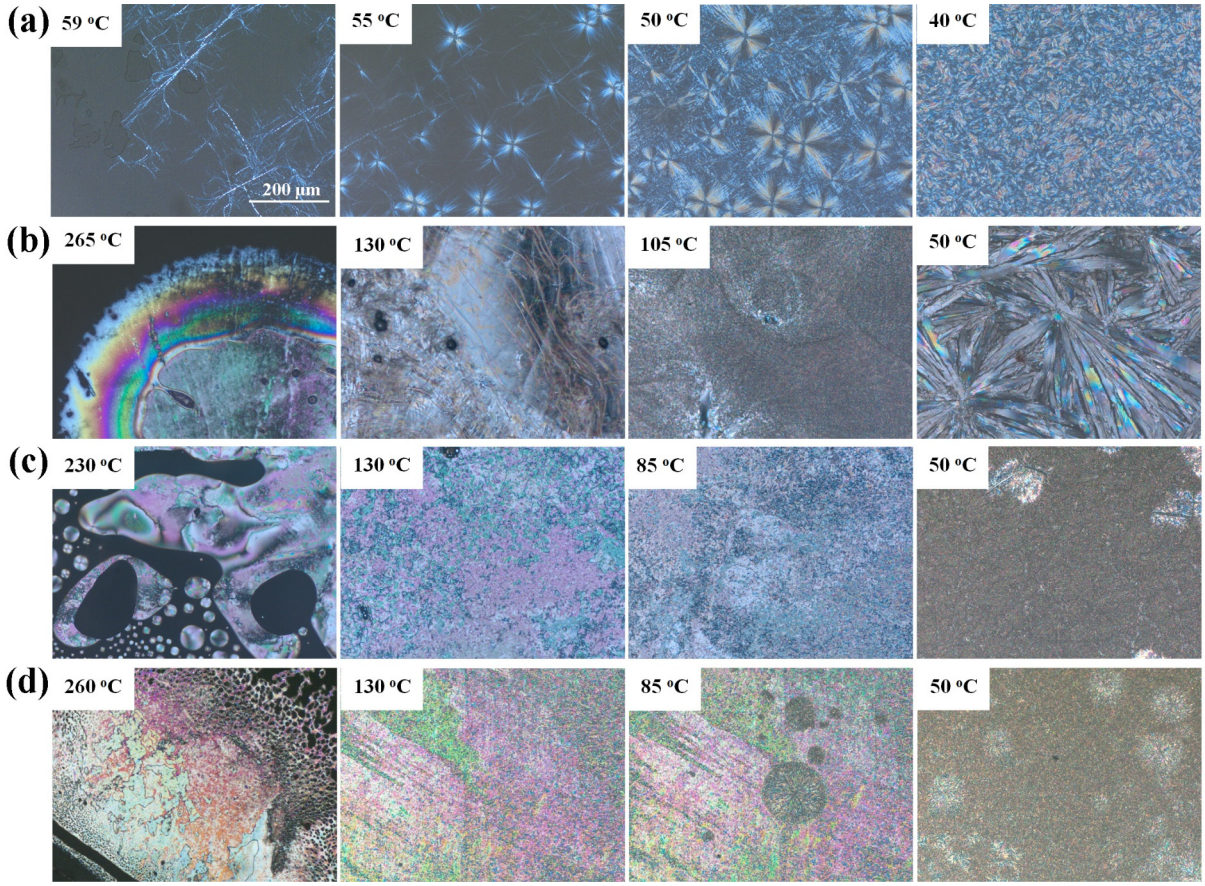

Figure 2. Polarizing optical microscopy photographs of thiophene bent-shaped molecules: (**a**) C6OP-6Th, (**b**) C5PP-6Th, (**c**) C5PPF(2)-6Th, and (**d**) C5PPF(3)-6Th at different temperatures during cooling cycle. All images were taken at the same magnification. The scale bar is 200 μm.

2.2. BP Behavior of Thiophene Bent-Shaped Molecules with Added Chiral Compounds

In previous studies, it was found that adding chiral additives to nonchiral bent-shaped LC molecules could induce the formation of BPs [20]. Thus, chiral dopant R811 was mixed with the thiophene molecules in increasing concentration to investigate the BP behavior. The chiral dopant R811 was added into the bent-shaped molecules in a definite proportion. A small amount of dichloromethane was added and stirred to mix the system homogeneously. Then, the dichloromethane was evaporated completely in an oven at 80 °C. The prepared mixtures were heated above the clear point and poured into the LC cells. The POM textures were observed during cooling or heating processes. For C5PP-6Th, the doping amount of R811 and the corresponding phase transition temperature of the mixture samples are shown in Table 2.

Table 2. The phase transition temperature for mixtures of C5PP-6Th and chiral dopant R811 in heating and cooling cycles.

Sample No.	R811 (wt%)	Heating (°C)	Cooling (°C)
A1	25	Cr 105.0 Ch 205.0 Iso	Iso 193.0 Ch 90.0 Cr
A2	30	Cr 105.0 Ch 190.0 Iso	Iso 178.0 Ch 85.0 Cr
A3	35	Cr 102.0 Ch 128.0 BP 174.0 Iso	Iso 170.0 BP 150.0 Ch 83.0 Cr
A4	40	Cr 100.0 Ch 130.0 BP 164.0 Iso	Iso 150.0 BP 130.0 Ch 100.0 Cr

Cr: Crystal; Ch: cholesteric phase; BP: blue phase; Iso: isotropic.

The POM textures of the samples at different temperatures are shown in Figures 3, S7 and S8. During the test, the heating or cooling rate was 0.5 °C min^{-1}. For sample A1, oily streaks of Ch were displayed when heating over the crystallization point (Figure S7a). As the sample was heated further to the clearing temperature, the oily striped texture disappeared and the POM presented a dark field. Similarly, only oily streaks of Ch were observed during the cooling process. In addition, the reflection color exhibited a blue shift with the decrease in temperature, which may contribute to the temperature sensitivity of the helical twist force of R811. When increasing the R811 doping amount to 30 wt%, the reflection color of Ch for sample A2 shifted to a short wavelength when compared with that of sample A1, as shown in Figure S7b. Thus, when the doping amount of R811 was less than 30 wt%, reversible phase transitions of Cr-to-Ch and Ch-to-Iso were observed. For sample A3, the oily striped texture disappeared, with blue fog being exhibited when increasing the temperature to 128 °C (Figure 3). Until the temperature rose to 160 °C, the blue fog texture changed to a cyan platelet texture. When further increasing the temperature to 174 °C, the phase transition to Iso accrued. During the cooling cycle, a local green platelet texture appeared at 170 °C and gradually expanded with the temperature decrease. A regular multidomain BP platelet texture was observed in the cyan reflection color at 162 °C, which then changed to a blue color at 160 °C. Further cooling to 150 °C, the reflection color of the POM texture changed to navy blue and oily streaks arose, indicating a phase transition from BP to Ch. Thus, BP existed in both heating and cooling processes, with corresponding temperature ranges of about 46 °C and 20 °C, respectively. For the POM textures of A3 observed in the LC cell with no parallel treatment (Figure S8), the phase transition processes were Ch 122.0 °C BP 165.0 °C Iso during the heating cycle, and Iso 160.5 °C BP 139.0 °C during the cooling cycle. The phase transition temperature slightly changed due to the different anchoring effects of the glass substrate. No obvious platelet textures were observed, which might be due to the high material viscosity hindering the growth of typical platelet textures of the BP. To further distinguish the phase state, the reflection spectra of sample A3 in the LC cell with parallel treatment during the heating and cooling processes were measured. The results are shown in Figure 4. The Ch is in a one-dimensional helical structure, while BPs are in double twist cylinder (DTC) structures. Therefore, the reflection wavelength of the Ch phase is usually smaller than that of BPs in the same material system. Then, in the reflection spectra, the peak position around 370 nm was assigned to the particular peak position for the Ch phase, while the reflection peak in the range of the 430–500 nm band was assigned to BPs. During the heating process, the reflection peak of Ch was significantly weakened at 130 °C. Due to the structural incompletion, the reflection peak of the BP was not obvious at this temperature. When further increasing the temperature to 140 °C, the reflection peak at 380 nm further decreased, while the reflection peak at 435 nm increased simultaneously. Subsequently, the reflection peak at about 370 nm completely disappeared, indicating phase transition completion from Ch to BP. The reflection peak of BP red-shifted from 435 nm to 454 nm and then disappeared with the increasing temperature. During the cooling process, a reflection peak at about 491 nm appeared and increased with the wavelength being shifted to the blue side with the decrease in temperature. After the decrease in temperature to below 152 °C, the peak intensity decreased rapidly to zero and the reflection peak at 370 nm appeared and increased at the same time. The results of the reflection spectra were almost consistent with the texture

changes observed with the POM. Due to the lack of a long-range-ordered periodic arrangement, the sample in BP III generally showed no obvious reflection peak. Moreover, the peak position of BP did not undergo a sudden change during the temperature-changing process, which helped to exclude the possibility of a phase transition from BP II to BP I [39]. Thus, the BP phase formed by C5PP-6Th doping with the chiral compound might be recognized as BP I. Moreover, it could be found that there was still a weak reflection peak of Ch during the heating process below 150 °C, indicating the coexistence of Ch and BPs, while during the cooling process at about 152 °C, the reflection peak of BP disappeared rapidly when the reflection peak of Ch appeared. Compared to the construction of a double-twisted DTC from a single-axis helical arrangement and the fabrication of long-range periodic supernanostructures, the DTC unwinding to form a single-axis helical arrangement might be easier. This might explain the different BP temperature ranges during the heating and cooling processes. For sample A4, only a blue fog texture was observed, and the clearing point decreased greatly. Moreover, crystallization occurred at 100 °C, which was caused by the excessive content of R811 that induced compatibility problems. Due to the biaxial nature of the molecules, the observed temperature range in this case was much wider than in traditional single uniaxial rod-like molecules mixed with chiral compounds. In addition, it was wider than the blue-phase temperature range observed in earlier biaxial molecular systems. Therefore, BP was achieved during the heating or cooling process by doping with the proper concentration of chiral compounds into the compound C5PP-6Th.

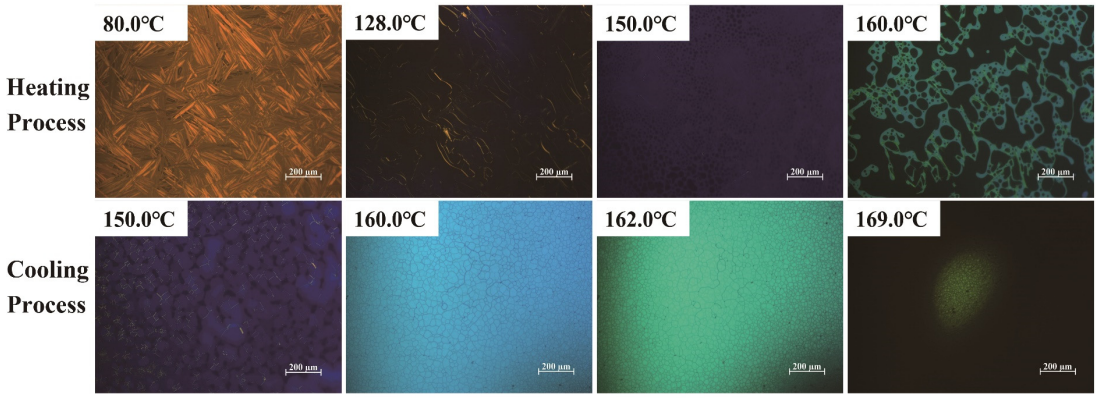

Figure 3. Typical POM textures of A3. The LC cells with parallel treatment. The scale bar is 200 μm.

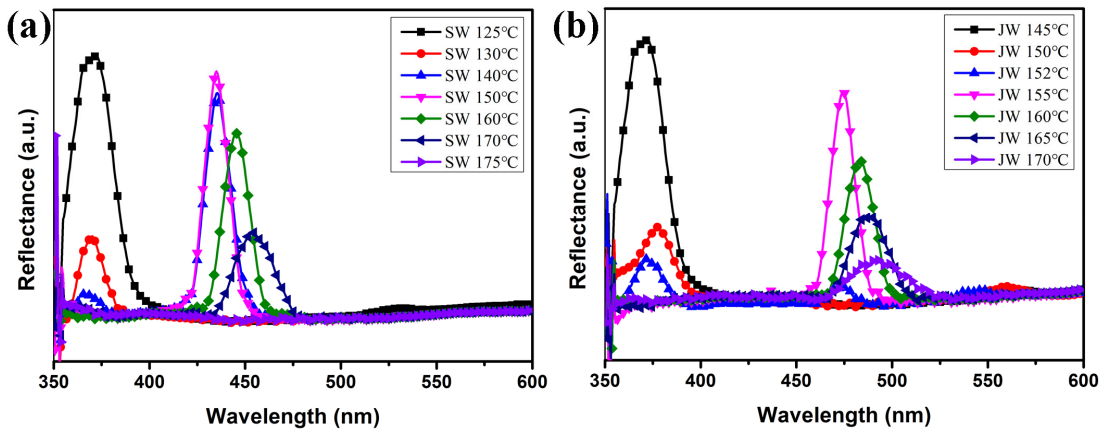

Figure 4. The reflection spectra of A3 in the LC cell with parallel treatment at different temperatures. (**a**) Heating process; (**b**) Cooling process.

For C5PPF(2)-6Th and C5PPF(3)-6Th, BP was not observed in either the heating or the cooling processes, regardless of the content of R811. Generally, a lateral fluoro-substituent is frequently employed in LC structures to modify the physical properties of LCs. As the

fluoro-substituent is larger than hydrogen, it may cause a significant steric effect when combined with the high polarity [40,41]. Generally, the coplanar of the organic molecules may be destroyed when introducing –F, –CN, or –Cl as a lateral group, and the molecular width will be increased [42,43]. Thus, it is hard for the neighboring molecules to form a close stack. In addition, the increase in intermolecular distance leads to a decrease in intermolecular lateral attraction, so it is unable to form a double-twist structure. As a result, BPs were not observed in these two molecular material systems.

2.3. Effect of Thiophene Bent-Shaped Molecules on BP Temperature Range

In order to investigate the effect of these bent-shaped compounds on the BP range, these molecules were doped into the BPLC host as testing samples and observed with a POM. The nematic liquid crystal mixture (SLC-4, cleaning point T_{NI} = 83.0 °C, Δε = 29.6 (at 25 °C), Δn= 0.235 (at 25 °C)) obtained from Shijiazhuang Slichem Display Material Co., Ltd., Shijiazhuang, China was used to prepare the host BPLC material. The prepared LC-1 host contained 89 % SLC-4 and 11 wt% Iso-$(6OBA)_2$, exhibiting a BP from 64.5 °C to 61.0 °C during the cooling process. By adding thiophene bent-shaped molecules into the LC-1 system with different concentrations, the BP temperature range was investigated. The samples were settled on the hot stage and heated from the Ch to the isotropic state; then, they were cooled from the Iso to Ch state with the same rate of 0.5 °C min^{-1}. The composition and phase transition temperature of the samples doped with C6OP-6Th are shown in Table 3. After the cooling process, every sample showed the typical BP texture and the microscopic pictures of sample 4 are presented in Figure 5 as a representative.

Table 3. Composition and phase transition temperature of the samples doped with C6OP-6Th.

Sample No.	Component (wt%)		Phase Transition Temperature		Temperature Range
	LC-1	C6OP-6Th	Iso-BP	BP-Ch	ΔT
0	100.0	0	64.5	61.0	3.5
1	99.5	0.5	63.2	54.5	8.7
2	99.0	1.0	61.3	49.7	11.6
3	98.0	2.0	58.9	45.7	13.2
4	97.0	3.0	57.4	45.0	12.4
5	96.0	4.0	56.2	44.6	11.6

ΔT is the blue-phase temperature range during cooling cycle.

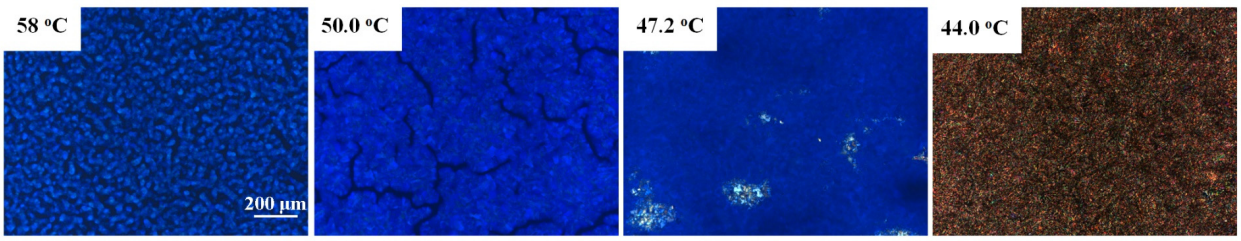

Figure 5. Polarizing optical microscopy photos of sample 4 at different temperatures during cooling cycle. All images were taken at the same magnification. The scale bar is 200 μm.

It can be seen from Table 3 that the addition of bent-shaped molecules was beneficial to the widening of the BP temperature range, which exhibited a tendency of first increasing and then decreasing with the increase in doping amount. The widest BP temperature range was about 13.2 °C at 2.0 wt% added amount. When the doping content was further increased, undissolved or precipitated crystals appeared locally in the sample. Because of the low melting point, the phase transition temperature of the samples decreased with the increase in the added amount of C6OP-6Th.

According to the above method, the BP temperature range was measured for the samples doped with the other three molecules in different doping amounts, as shown in

Figure 6. Due to the enhancement of the rigid molecular structure, the solubility of the corresponding derivatives in LC-1 was limited. When the added amount exceeded 2 wt%, obvious precipitates or insoluble substances appeared. In addition, the phase transition temperature of the doped samples increased slightly with the increase in bent-shaped molecular addition, as did the high liquid-crystalline phase temperature. For these threthe e molecules, the optimal doping amount in LC-1 was different. For C5PP-6Th, the widest BP temperature range of 18.4 °C was obtained at 1.0 wt% added amount. For C5PPF(2)-6Th and C5PPF(3)-6Th, the optimal amount was the same, 1.5 wt%, broadening the BP to 24.1 °C and 20.5 °C, respectively. When the content exceeded a certain level, bent-core molecules may have increased the energy of the double-twisted cylinder arrangement of the rod-like LC molecules and, thus, decreased the stability of the BP. Through a comparison of the experimental results, the lateral F moiety substitute definitely enhanced the BP broadening effect. The solubility improvement in LC-1 benefiting from –F might also take effect. Moreover, as its ortho-substitution around the ester linkage of the molecular skeleton decreased the clearing point temperature dramatically, the position of –F also made a difference [41].

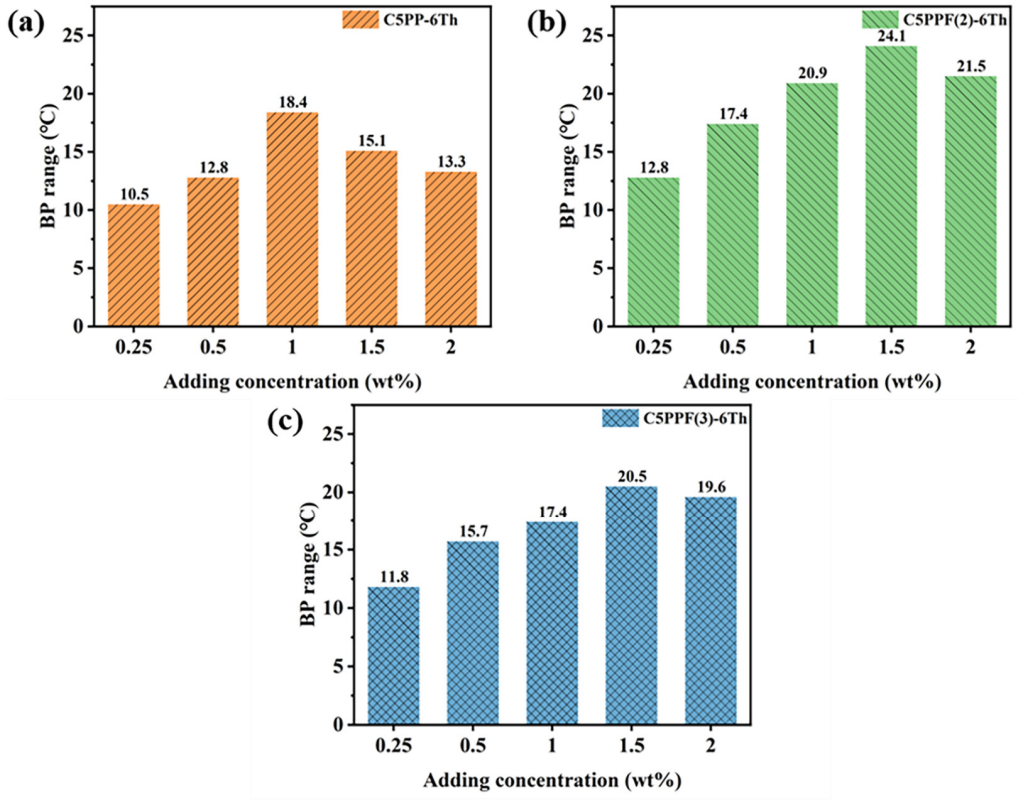

Figure 6. The BP temperature range of samples doped with thiophene bent-shaped molecules in LC-1. (**a**) Samples doped with C5PP-6Th; (**b**) Samples doped with C5PPF(2)-6Th; (**c**) Samples doped with C5PPF(3)-6Th.

To study the influence of molecular structure on their mesogenic behavior and BP thermodynamic stability, the bent-shaped molecules were calculated with density functional theory (DFT) using the GAUSSIAN 09 program, in which the FOPT calculation type with the B3LYP method was employed for the nonlocal correlation and the 6-31G basis set was used for geometry optimizations [38]. The equilibrium geometries corresponding to the global minimum optimized structure of each compound are shown in Figure 7. The optimized structural parameters of all the molecules are summarized in Table 4. As is known, one of the major structural requirements for organic compounds exhibiting mesophase behavior is that the molecules must have a large length-to-width ratio (L/W

ratio), usually greater than 4. Based on the calculated L/W ratios, we can easily understand that C6O-6Th exhibits no mesogenic properties as the L/W ratio is less than 4.

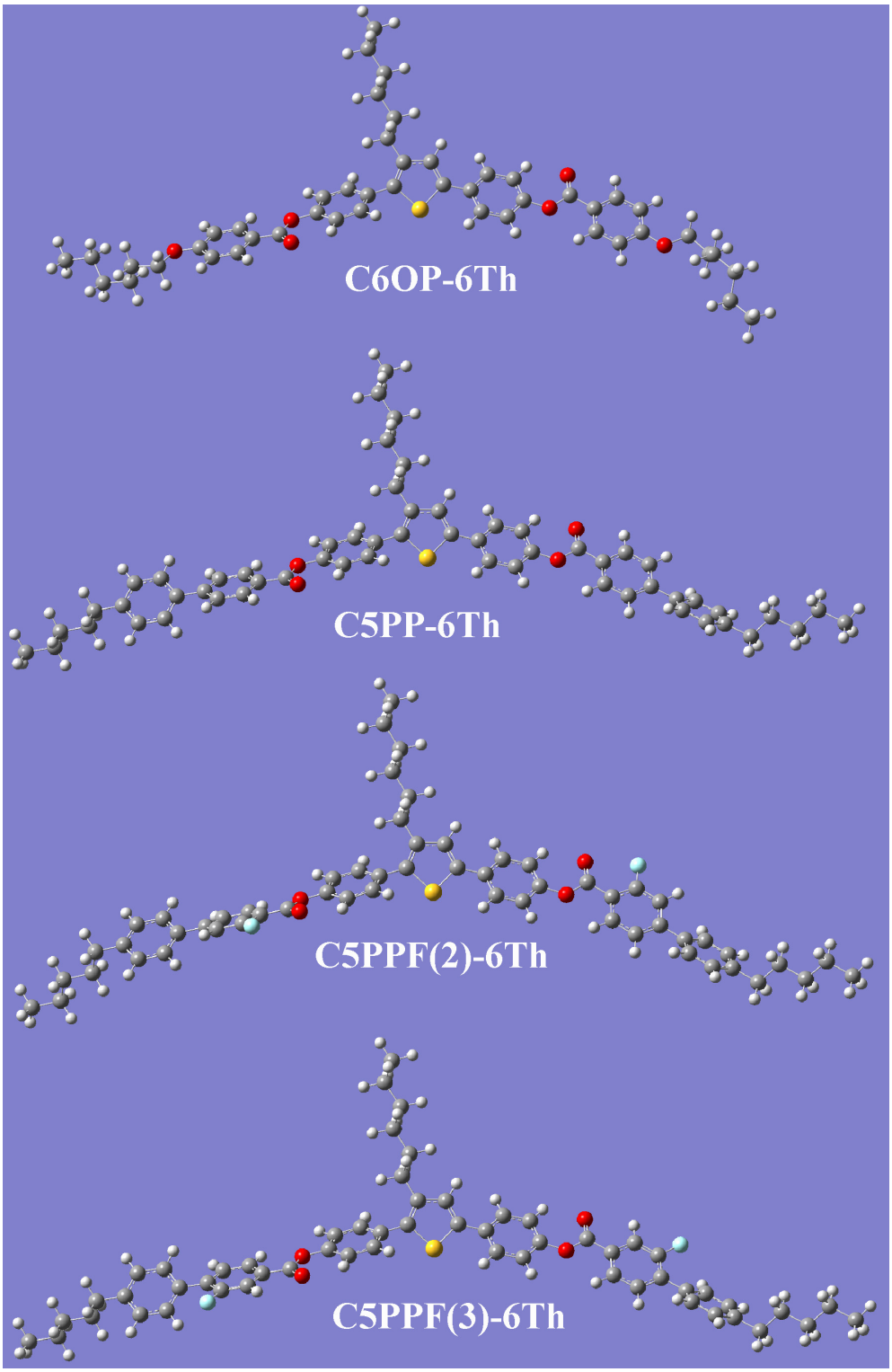

Figure 7. The typical optimized molecular conformations corresponding to the global minimum optimized structure of the bent-shaped molecules. Grey, red, yellow, white, and cyan balls represent carbon, oxygen, sulfur, hydrogen, fluorine atoms respectively.

Table 4. The molecular parameters calculated by using GAUSSIAN 09 program at the B3LYP/6-31G level for the 3-hexyl-2,5-disubstituted thiophene derivatives.

Sample. No	E(B3LYP)	Dipole Moment	Length	Width	L/W
C6OP-6Th	2711.8	0.95	39.24	11.00	3.57
C5PP-6Th	2944.8	1.52	45.34	11.03	4.11
C5PPF(2)-6Th	3143.2	3.67	45.22	11.21	4.03
C5PPF(3)-6Th	3143.3	2.19	45.32	11.32	4.00

As has been reported previously, bent-shaped molecules can induce the double-twisted helical arrangement of LC molecules due to their special molecular twist configuration and biaxiality, which is conducive to the transfer of chirality [22]. Thus, compared with C6OP-6Th, the molecules C5PP-6Th, C5PPF(2)-6Th, and C5PPF(3)-6Th with strong biaxiality exhibited a significant effect on stabilizing the BP at low concentrations. From the simulation calculation results, it can be seen that the presence and position of fluorine atoms have a significant impact on the value of molecular dipole moments. In accordance with the experiments, the BP broadening effect was improved with the increase in the dipole moments. Thus, it could be supposed that the molecular dipole moment might be a key factor affecting the structural stability of the BP. Moreover, the addition of bent-shaped molecules was proven to modify the elastic constant and decrease the ratio of K_{33} and K_{11} of LC materials. Thus, the free energy of the system declines and the DTC nanostructure of the BP can be stabilized [28]. Theoretical research shows that K_{33}/K_{11} is closely related to the value of the length/diameter ratio, which reduces with the decrease in aspect ratio [44]. In the case of other identical structures, the introduction of fluorine atom side-substituting groups at different positions could reduce the molecular effective aspect ratio slightly, as summarized in Table 4. Therefore, BPLC materials with a temperature range greater than 20 °C were obtained by adding a small amount of C5PP(2)-6Th to a BPLC host.

3. Conclusions

In summary, four thiophene bent-shaped molecules with different molecular long-axis lengths or lateral substituent structures were prepared. The effect of molecular structure on the phase transition behavior was investigated. LC phases were achieved for the molecules with more benzene rings on the long axis. By the lateral F moiety situated around the ester linkage of the molecular skeleton, the phase transition temperatures from crystal state to nematic phase were decreased. The clearing point temperature reduced by 30 °C due to F-ortho-substitution. By doping C5PP-6Th with R811 in 35 wt%, BPs were achieved during both heating and cooling processes, with corresponding temperature ranges of about 46 °C and 20 °C, respectively. In contrast, for C5PPF(2)-6Th and C5PPF(3)-6Th, only Ch was observed no matter how many chiral compounds were added, which might have contributed to the steric effect of the lateral F substitution that inhibited the formation of DTCs of the BP. The effect of these bent-shaped compounds on the BP range was studied by doping them into a BPLC host. The BP temperature range first widened and then narrowed with the increase in the doping concentration due to the limited solubility. The sample with 1.5 wt% proportion of C5PPF(2)-6Th exhibited the widest BP temperature range up to 24 °C, and the transition temperature was close to room temperature. Through the theoretical calculation of density functional theory, the optimized structural parameters of the molecules were obtained, which explained their mesogenic properties using the calculated length-to-width ratio. Moreover, through the analysis of experimental and computational results, the molecular dipole moment might be a key factor affecting the structural stability of the BP in a bent-shaped-molecule-doped LC material system. The study may provide new insights for the molecular design of bent-shaped molecules and has excellent application prospects in novel BPLC materials.

Supplementary Materials: The following supporting information can be downloaded at: https://www.mdpi.com/article/10.3390/cryst13060916/s1, Scheme S1: Synthetic route of the studied compounds. Reagents and conditions: (A) $Pd(PPh_3)_4$, aq. K_2CO_3, alcohol, toluene, 80 °C; (B) BBr_3, RT; (C) DCC, DMAP, CH_2Cl_2, RT: Figure S1: The ^{1}H NMR (400MHz, $CDCl_3$) spectra of C6O-6Th; Figure S2: The ^{1}H NMR (400MHz, $CDCl_3$) spectra of C5PP-6Th; Figure S3: The ^{1}H NMR (400MHz, $CDCl_3$) spectra of C5PPF(2)-6Th; Figure S4: The ^{1}H NMR (400MHz, $CDCl_3$) spectra of C5PPF(3)-6Th; Figure S5: The DSC thermograms of compound (a) C6OP-6Th, (b) C5PP-6Th, (c) C5PPF(2)-6Th and (d) C5PPF(3)-6Th with the heating as well as cooling scans at the rate of 10 °C min^{-1}; Figure S6: The chemical structure of chiral dopant R811 and Iso-$(6OBA)_2$; Figure S7: Typical POM textures in LC cells with parallel treatment of A1, A2 and A4 for C5PP-6Th blended with different contents of chiral dopant R811. The scale bar is 200 μm; and Figure S8: Typical POM textures in LC cells with no parallel treatment of A3. The scale bar is 100 μm. Reference [45] is cited in the Supplementary Materials.

Author Contributions: The manuscript was written by M.W. and H.S. The experiments and analyses were conducted by M.W., H.S., C.W. and B.L. The molecular simulation calculation was conducted by Z.W. and H.Y. supervised the project and finalized the manuscript. All authors have read and agreed to the published version of the manuscript.

Funding: This work was supported by the National Natural Science Foundation of China (NSFC) (Grant Nos. 52003293, 51927806), the Fundamental Research Funds for the Central Universities (Grant No: 2022YQJD07), and the Innovation Training Program for University Students of China University of Mining and Technology-Beijing (Grant Nos: 5200030826, 51927806).

Data Availability Statement: The raw/processed data required to reproduce these findings cannot be shared at this time as the data also forms part of an ongoing study.

Conflicts of Interest: The authors declare no conflict of interest.

References

1. Bisoyi, H.K.; Li, Q. Liquid Crystals: Versatile Self-Organized Smart Soft Materials. *Chem. Rev.* **2022**, *122*, 4887–4926. [CrossRef] [PubMed]
2. Wang, L.; Urbas, A.M.; Li, Q. Nature-Inspired Emerging Chiral Liquid Crystal Nanostructures: From Molecular Self-Assembly to DNA Mesophase and Nanocolloids. *Adv. Mater.* **2020**, *32*, 1801335. [CrossRef]
3. Zheng, Z.-G.; Yuan, C.-L.; Hu, W.; Bisoyi, H.K.; Tang, M.-J.; Liu, Z.; Sun, P.-Z.; Yang, W.-Q.; Wang, X.-Q.; Shen, D.; et al. Light-Patterned Crystallographic Direction of a Self-Organized 3D Soft Photonic Crystal. *Adv. Mater.* **2017**, *29*, 1703165. [CrossRef] [PubMed]
4. Liu, J.; Liu, W.; Guan, B.; Wang, B.; Shi, L.; Jin, F.; Zheng, Z.; Wang, J.; Ikeda, T.; Jiang, L. Diffusionless transformation of soft cubic superstructure from amorphous to simple cubic and body-centered cubic phases. *Nat. Commun.* **2021**, *12*, 3477. [CrossRef] [PubMed]
5. Gandhi, S.S.; Chien, L.-C. Unraveling the Mystery of the Blue Fog: Structure, Properties, and Applications of Amorphous Blue Phase III. *Adv. Mater.* **2017**, *29*, 1704296. [CrossRef] [PubMed]
6. Yang, J.; Zhao, W.; He, W.; Yang, Z.; Wang, D.; Cao, H. Liquid crystalline blue phase materials with three-dimensional nanostructures. *J. Mater. Chem. C* **2019**, *7*, 13352–13366. [CrossRef]
7. Wang, H.; Zhou, H.; He, W.; Yang, Z.; Cao, H.; Wang, D.; Li, Y. Research Progress on Blue-Phase Liquid Crystals for Pattern Replication Applications. *Materials* **2023**, *16*, 194. [CrossRef]
8. Rahman, M.D.A.; Said, S.M.; Balamurugan, S. Blue phase liquid crystal: Strategies for phase stabilization and device development. *Sci. Technol. Adv. Mater.* **2015**, *16*, 033501. [CrossRef]
9. Yoshizawa, A. Material design for blue phase liquid crystals and their electro-optical effects. *RSC Adv.* **2013**, *3*, 25475–25497. [CrossRef]
10. Coles, H.J.; Pivnenko, M.N. Liquid crystal 'blue phases' with a wide temperature range. *Nature* **2005**, *436*, 997–1000. [CrossRef]
11. Hu, W.; Wang, L.; Wang, M.; Zhong, T.; Wang, Q.; Zhang, L.; Chen, F.; Li, K.; Miao, Z.; Yang, D.; et al. Ultrastable liquid crystalline blue phase from molecular synergistic self-assembly. *Nat. Commun.* **2021**, *12*, 1440. [CrossRef] [PubMed]
12. Yoshizawa, A.; Sato, M.; Rokunohe, J. A blue phase observed for a novel chiral compound possessing molecular biaxiality. *J. Mater. Chem.* **2005**, *15*, 3285–3290. [CrossRef]
13. Shi, Y.; Wang, X.W.; Wei, J.; Yang, H.; Guo, J.B. Stabilization of blue phases by hydrogen-bonded bent-shaped and T-shaped molecules featuring a branched terminal group. *Soft Matter* **2013**, *9*, 10186–10195. [CrossRef]
14. Yoshizawa, A.; Kogawa, Y.; Kobayashi, K.; Takanishi, Y.; Yamamoto, J. A binaphthyl derivative with a wide temperature range of a blue phase. *J. Mater. Chem.* **2009**, *19*, 5759–5764. [CrossRef]

15. Etxebarria, J.; Ros, M.B. Bent-core liquid crystals in the route to functional materials. *J. Mater. Chem.* **2008**, *18*, 2919–2926. [CrossRef]
16. Jakli, A. Liquid crystals of the twenty-first century—Nematic phase of bent-core molecules. *Liq. Cryst. Rev.* **2013**, *1*, 65–82. [CrossRef]
17. Abberley, J.P.; Killah, R.; Walker, R.; Storey, J.M.D.; Imrie, C.T.; Salamonczyk, M.; Zhu, C.; Gorecka, E.; Pociecha, D. Heliconical smectic phases formed by achiral molecules. *Nat. Commun.* **2018**, *9*, 228. [CrossRef]
18. Jákli, A.; Nastishin, Y.; Lavrentovich, O.D. Defects in bent-core liquid crystals. *Liq. Cryst. Rev.* **2022**. [CrossRef]
19. Nakata, M.; Takanishi, Y.; Watanabe, J.; Takezoe, H. Blue phases induced by doping chiral nematic liquid crystals with nonchiral molecules. *Phys. Rev. E* **2003**, *68*, 041710. [CrossRef]
20. Lee, M.; Hur, S.-T.; Higuchi, H.; Song, K.; Choi, S.-W.; Kikuchi, H. Liquid crystalline blue phase I observed for a bent-core molecule and its electro-optical performance. *J. Mater. Chem.* **2010**, *20*, 5813–5816. [CrossRef]
21. Ocak, H.; Bilgin-Eran, B.; Prehm, M.; Schymura, S.; Lagerwall, J.P.F.; Tschierske, C. Effects of chain branching and chirality on liquid crystalline phases of bent-core molecules: Blue phases, de Vries transitions and switching of diastereomeric states. *Soft Matter* **2011**, *7*, 8266–8280. [CrossRef]
22. Yoshizawa, A. Liquid crystal supermolecules stabilizing an optically isotropic phase with frustrated molecular organization. *Polym. J.* **2012**, *44*, 490–502. [CrossRef]
23. Wang, L.; He, W.L.; Xiao, X.; Yang, Q.; Li, B.R.; Yang, P.Y.; Yang, H. Wide blue phase range and electro-optical performances of liquid crystalline composites doped with thiophene-based mesogens. *J. Mater. Chem.* **2012**, *22*, 2383–2386. [CrossRef]
24. Wang, L.; Yu, L.; Xiao, X.; Wang, Z.; Yang, P.; He, W.; Yang, H. Effects of 1,3,4-oxadiazoles with different rigid cores on the thermal and electro-optical performances of liquid crystalline blue phases. *Liq. Cryst.* **2012**, *39*, 629–638. [CrossRef]
25. Punjani, V.; Mohiuddin, G.; Kaur, S.; Choudhury, A.R.; Paladugu, S.; Dhara, S.; Ghosh, S.; Pal, S.K. Chiral Bent-Shaped Molecules Exhibiting Unusually Wide Range of Blue Liquid-Crystalline Phases and Multistimuli-Responsive Behavior. *Chem.—Eur. J.* **2020**, *26*, 5859–5871. [CrossRef]
26. Khan, R.K.; Mohiuddin, G.; Begum, N.; Turlapati, S.; Nandiraju, R.V.S.; Debbarma, B.K.; Ghosh, S. Extremely High Kerr Constant and Low Operating Voltage in a Stable Room-Temperature Blue Phase III Derived from Three-Ring-Based Bent-Core Molecules. *ACS Appl. Mater. Interfaces* **2022**, *14*, 42628–42634. [CrossRef]
27. Alexander, G.; Yeomans, J. Stabilizing the blue phases. *Phys. Rev. E* **2006**, *74*, 061706. [CrossRef]
28. Hur, S.-T.; Gim, M.-J.; Yoo, H.-J.; Choi, S.-W.; Takezoe, H. Investigation for correlation between elastic constant and thermal stability of liquid crystalline blue phase I. *Soft Matter* **2011**, *7*, 8800–8803. [CrossRef]
29. Bisoyi, H.K.; Li, Q. Light -Driven Liquid Crystalline Materials: From Photo -Induced Phase Transitions and Property Modulations to Applications. *Chem. Rev.* **2016**, *116*, 15089–15166. [CrossRef]
30. Begum, N.; Kaur, S.; Mohiuddin, G.; Nandi, R.; Gupta, S.P.; Rao, N.V.S.; Pal, S.K. Structural Understanding, Photoswitchability, and Supergelation of a New Class of Four Ring-Based Bent-Shaped Liquid Crystal. *J. Phys. Chem. B* **2019**, *123*, 4443–4451. [CrossRef]
31. Wang, H.F.; Zheng, Z.G.; Shen, D. Blue phase liquid crystals induced by bent-shaped molecules based on 1,3,4-oxadiazole derivatives. *Liq. Cryst.* **2012**, *39*, 99–103. [CrossRef]
32. Kaur, S.; Punjani, V.; Yadav, N.; Barthakur, A.; Baghla, A.; Dhara, S.; Pal, S.K. Chemical and physical aspects of recent bent-shaped liquid crystals exhibiting chiral and achiral mesophases. *Liq. Cryst.* **2022**, *49*, 1078–1146. [CrossRef]
33. Qi, R.-Z.; Shi, Q.-K.; Wang, Y.-F.; Yang, J.-Y.; Kang, J.-T.; Jia, Y.-G. Effect of terminal chain length on mesomorphic behavior and selective reflection of blue phase liquid crystals. *Liq. Cryst.* **2022**, *49*, 1689–1697. [CrossRef]
34. Wang, L.; He, W.; Wang, M.; Wei, M.; Sun, J.; Chen, X.; Yang, H. Effects of symmetrically 2,5-disubstituted 1,3,4-oxadiazoles on the temperature range of liquid crystalline blue phases: A systematic study. *Liq. Cryst.* **2013**, *40*, 354–367. [CrossRef]
35. Han, J. 1,3,4-Oxadiazole based liquid crystals. *J. Mater. Chem. C* **2013**, *1*, 7779–7797. [CrossRef]
36. Reddy, Y.S.K.; Lobo, N.P.; Sampath, S.; Narasimhaswamy, T. Morphology, Mesophase, and Molecular Order of 3-Hexyl Thiophene-Based π-Conjugated Mesogens. *J. Phys. Chem. C* **2016**, *120*, 17960–17971. [CrossRef]
37. Bajzíková, K.; Veselý, J.; Kozmík, V.; Svoboda, J.; Novotná, V.; Pociecha, D. Diphenylthiophenes as central part for the design of bent-core liquid crystalline compounds. *J. Mol. Liq.* **2018**, *267*, 496–503. [CrossRef]
38. Han, Z.-Y.; Kun, S.-Q.; Kang, J.-T.; Jia, Y.-G. New (-)-menthol-based blue phase liquid crystals with different polar substituents in the terminal group: Synthesis, mesophase behaviors, and DFT calculations. *J. Mol. Struct.* **2022**, *1263*, 133147. [CrossRef]
39. Yoshida, H.; Anucha, K.; Ogawa, Y.; Kawata, Y.; Ozaki, M.; Fukuda, J.-i.; Kikuchi, H. Bragg reflection band width and optical rotatory dispersion of cubic blue-phase liquid crystals. *Phys. Rev. E* **2016**, *94*, 042703. [CrossRef]
40. Hird, M. Fluorinated liquid crystals—Properties and applications. *Chem. Soc. Rev.* **2007**, *36*, 2070–2095. [CrossRef]
41. Tschierske, C. Fluorinated Liquid Crystals: Design of Soft Nanostructures and Increased Complexity of Self-Assembly by Perfluorinated Segments. In *Liquid Crystals: Materials Design and Self-Assembly*; Tschierske, C., Ed.; Springer: Berlin/Heidelberg, Germany, 2012; Volume 318, pp. 1–108.
42. Cigl, M.; Jurok, R.; Hampl, F.; Svoboda, J.; Podoliak, N.; Novotna, V. Lateral substituted phenyl biphenylcarboxylates—Non-chiral analogues of ferroelectric liquid crystals. *Liq. Cryst.* **2020**, *47*, 768–776. [CrossRef]

43. Harkins, R.; Tauscher, T.; Nguyen, J.; Lewis, S.; Adamo, F.C.; Pisani, M.; Hermida-Merino, D.; Samulski, E.T.; Vita, F.; Francescangeli, O.; et al. Biaxial ordering in the supercooled nematic phase of bent-core mesogens: Effects of molecular symmetry and outer wing lateral groups. *Liq. Cryst.* **2020**, *47*, 1986–1998. [CrossRef]
44. Chen, H.-Y.; Liu, H.-H.; Lai, J.-L.; Chiu, C.-H.; Chou, J.-Y. Relation between physical parameters and thermal stability of liquid-crystal blue phase. *Appl. Phys. Lett.* **2010**, *97*, 181919. [CrossRef]
45. Cheng, X.H.; Dong, X.; Zheng, T.; Ye, H.; Wei, G.H. Synthesis and Mesomorphic Behavior of 3-Alkyl-2,5- bis[p-(hexa-2,4-dienoyloxy)phenyl]-Thiophene Derivatives. *Chin. J. Chem.* **2008**, *26*, 146–149. [CrossRef]

Disclaimer/Publisher's Note: The statements, opinions and data contained in all publications are solely those of the individual author(s) and contributor(s) and not of MDPI and/or the editor(s). MDPI and/or the editor(s) disclaim responsibility for any injury to people or property resulting from any ideas, methods, instructions or products referred to in the content.